For example, this threshold is about 60°C in Lower Jurassic sediments of the Paris Basin, but is 115°C in Mio-Pliocene sediments of the Los Angeles Basin. The temperature and depth scales in Figure 12.37 correspond to a relatively high geothermal gradient (40°C/km). Reaction rates also depend upon the type of kerogen involved. Labile reactive kerogen (Type I) reacts at relatively low temperatures; refractory Type III can require substantially higher temperatures for petroleum generation (as high as 250°C). Since long aliphatic chains are unstable at these temperatures, the principal product of Type III kerogen is methane.

12.7.3.2 Migration and post-generation compositional evolution

Most petroleum source rocks are fine-grained. Subjected to the pressure of burial, their porosities are typically quite low; hence liquid and gaseous hydrocarbons are expelled once the source rock becomes saturated. Being less dense than both rock and water, petroleum and gas tend to migrate upward. The mechanisms of migration of hydrocarbons are not fully understood, but probably involve both passage through microfractures and diffusion through the kerogen matrix. Migration will continue until the petroleum reaches an impermeable barrier, a "trap", or the surface. From the standpoint of economic recovery, the ideal situation is a trap, such as a clay-rich sediment, overlying a porous and permeable "reservoir" rock such as sandstone. Expulsion efficiencies vary with kerogen type. In Type I kerogen, nearly all the oil can be expelled from the source rock. In Type III kerogen and coal, however, most or all of the oil may remain trapped in the source rock and be ultimately cracked to gas.

The quantity and quality of the petroleum generated depends largely on the type of organic matter. Since petroleum tends to migrate out of the source rock as it is created, it is difficult to judge the amount of petroleum generated from field studies. However, both mass balance calculations on natural depth sequences and laboratory pyrolysis experiments on immature kerogen give some indication of the petroleum generation potential (Tissot and Welte, 1984; Rullkötter, 1993). Type I kerogen yields up to 80% light hydrocarbons upon pyrolysis. Mass balance studies of Type II kerogen indicate a hydrocarbon generation potential of up to 60%. Type III kerogens yield much less hydrocarbon upon pyrolysis (<15%).

Chemical changes may occur in several ways during and after migration. Fractionation during migration can occur as a result of the differing diffusivity and viscosity of hydrocarbons: light hydrocarbons are more diffusive and less viscous than heavy ones. As a result, they will migrate more readily, and the hydrocarbons in a reservoir are often enriched in the light fraction compared with the source rock. Asphaltenes are insoluble in light hydrocarbons and may precipitate as a consequence of this process. Polar constituents in oil, asphaltenes and resins, may be absorbed by mineral surfaces and are less readily expelled from the source rock, resulting in a depletion in these components in oil in reservoir rocks compared with source rock bitumen. The more water-soluble components of petroleum may dissolve in water either flowing through a reservoir or encountered by migrating petroleum. This process, called *water washing,* will deplete the petroleum in these water-soluble components. Aerobic bacteria encountered by petroleum can metabolize petroleum components, in a process called *biodegradation*. Long, unbranched alkyl chains are preferentially attacked, followed by branched chains, cycloalkanes, and acyclic isoprenoids. Aromatic steroids are the least affected. Finally, further thermal evolution can occur after migration, resulting in an increase in methane and aromatic components at the expense of aliphatic chains.

12.7.3.3 Composition of crude oils

Figure 12.38 summarizes the compositions of crude oils. Average "producible" crude oils contain 57% aliphatic hydrocarbons (with a slight dominance of acyclic over cyclic), 29% aromatic hydrocarbons, and 14% resins and asphaltenes. On an elemental basis, it consists approximately of 82–87% C, 12–15% H, 0.1–5% each of S and O, and 0.1–1.5% N by weight. On an atomic basis, this corresponds to a C:H:S:O:N ratio of 100:190:2.5:4:1.5. The distribution of n-alkanes differs widely between various types of crudes, as may be seen in Figure 12.39. Among cycloalkanes,

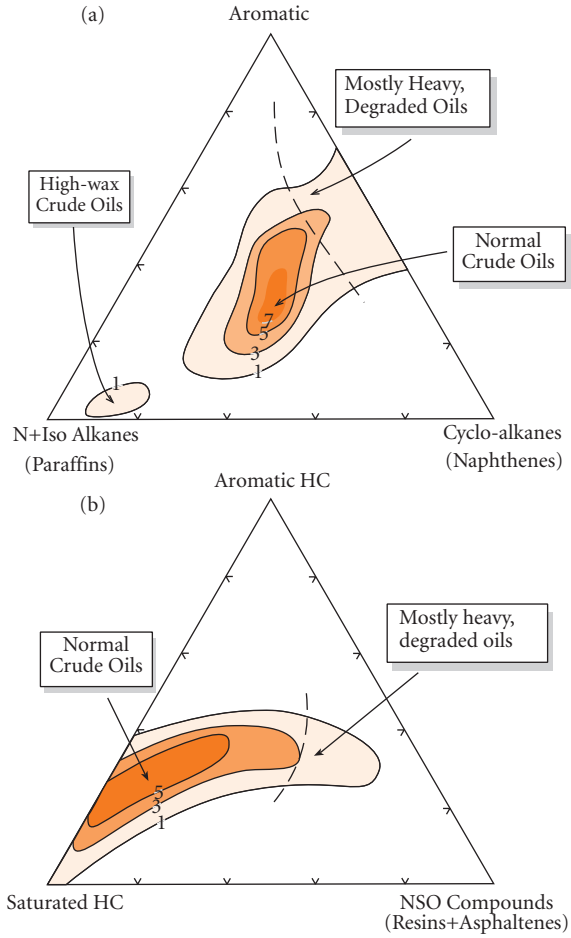

Figure 12.38 Ternary diagrams representing the composition of crude oils. (a) Isofrequency contours of hydrocarbons boiling above 210°C in 541 crude oils divided between aromatics, cyclo-alkanes, and n- and isoalkanes. (b) Isofrequency contours of saturated hydrocarbons, aromatic hydrocarbons, and NSO compounds (wt. percent in the fraction boiling above 210°C) in 636 crude oils. Tissot and Welte (1984). With kind permission from Springer Science+Business Media B.V.

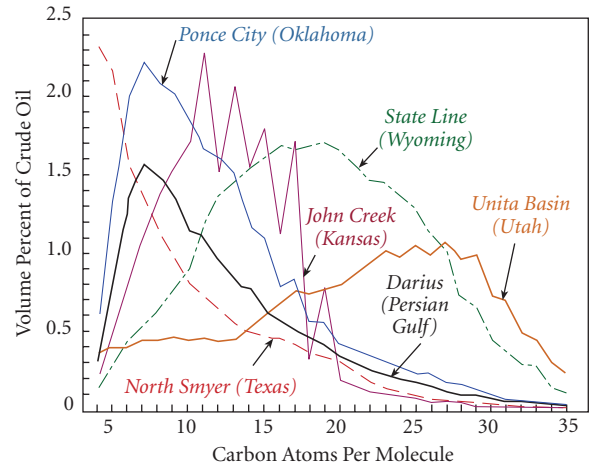

Figure 12.39 Distribution of n-alkanes in different crude oils. Tissot and Welte (1984). With kind permission from Springer Science+Business Media B.V.

those with 2 to 4 rings generally predominate. Alkylated compounds dominate the aromatic fraction; those with one to three additional carbons are most common. Aromatics decrease in abundance with increasing number of rings, so that benzene derivatives (one ring) are most common, followed by naphthalenes (two rings), and so on. Molecules containing both saturated and unsaturated rings (naphthnoaromatics) are also present, typically in an abundance of 5 wt.%. Upon primary distillation, typical crude oil yields 27 volume percent gasoline (C_4–C_{10} compounds), 13% kerosene (C_{11}–C_{13}), 12% diesel fuel (C_{14}–C_{18}), 10% heavy gas oils (e.g., heating oil) (C_{19}–C_{25}), and 20% lubricating oil (C_{26}–C_{40}) (Royal Dutch Shell, 1983). The ratio of these products can be changed by further refining processes such as solvent extraction, thermal cracking, catalytic cracking, and so on, so that, for example, the gasoline yield can be as high as 50%.

12.7.4 Compositional evolution of coal

Coal, as we noted earlier, forms from organic-rich sediments typically deposited in swamps. Coal evolution is a process of selective preservation of some resistant organic remains, which generally constitute a minor fraction of the original mass, followed by minor reorganization of the biopolymers that survive (Hatcher and Clifford, 1997). Two types of coals are recognized: sapropelic and humic. Humic coals are by far the most common. They are bright, usually stratified, rich in aromatics, and composed primarily of the remains of higher plants. Less common sapropelic coals are dull, rarely stratified, and derived from lipid-rich organic matter such as the remains of algae (boghead coals or torbanites) or spores (cannel coals). The primary maceral

group of humic coals is vitrinite, while that of sapropelic coals is exinite.

The evolution of coal, illustrated in Figures 12.40 and 12.41, is generally broken down into two phases: *peatification* and *coalification*. Coalification is subdivided into *biochemical* and *geochemical* stages. Together, peatification and the biochemical stage of coalification are equivalent to diagenesis, while the geochemical stage of coalification is comparable to catagenesis. During peatification, bacterial and fungal attack results in depolymerization and removal of functional groups from the original biomolecules (Figure 12.41). This process is begun by aerobic organisms and continued by anaerobic bacteria once conditions become reducing. This is accompanied by the evolution of various gases, primarily CO_2 and H_2O with lesser amounts of NH_3, N_2, and CH_4, and condensation of the degradation products into humic substances. As in diagenesis, the concentrations of the most labile components decrease, while those of more refractory ones increase. The latter include lignins and tannins, and lipids derived from leaves, spores, pollen, fruit, and resin. Another important process during peatification is compaction and expulsion of water.

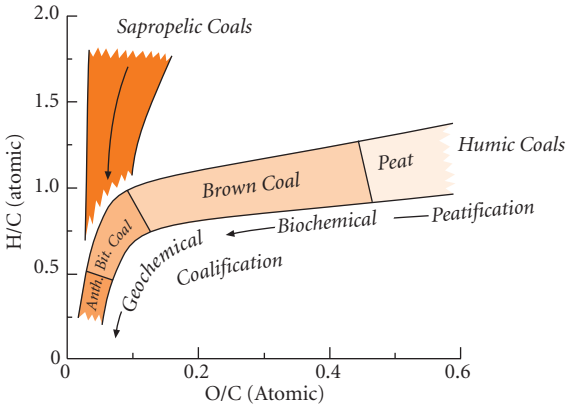

Figure 12.40 Chemical evolution of coals. Killops and Killops (2005). With permission from John Wiley & Sons.

During biochemical coalification, continued loss of functional groups drives the O/C ratio to lower values with only a slight decrease in H/C ratio. Remaining labile components are metabolized and refractory material continues to condense to aromatic-dominated structures (Figure 12.41). The final product of the diagenetic phase is *brown coal*, which contains 50–60% C and 5–7% H. This material may be accompanied by a small bitumen fraction, derived primarily from lipid components.

Temperature and pressure increase with burial and this initiates the geochemical stage of coalification. Coal at this stage contains 1–2% N and generally less than 1% S. Continued compaction results in a continued decrease in the water present. Loss of functional groups further reduces the O/C ratio with only a minor decrease in the H/C ratio. By the time the O/C ratio reaches 0.1, most of the functional groups have been lost. The

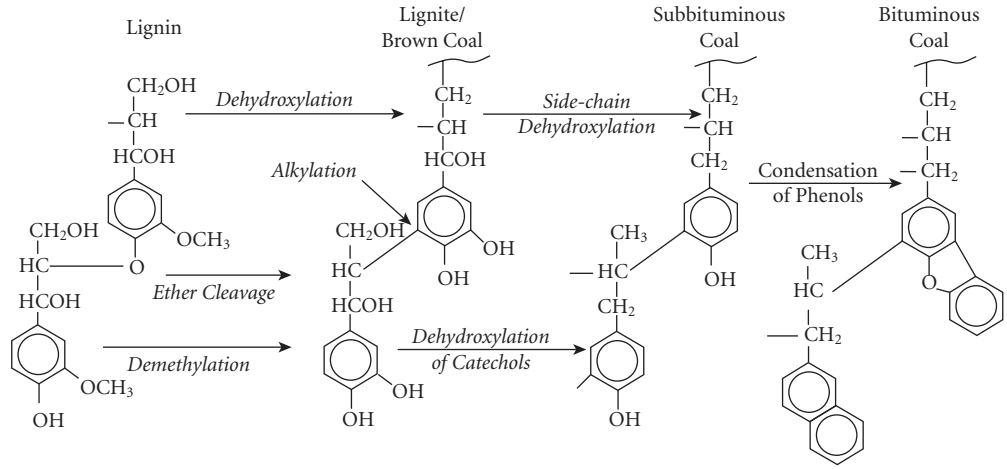

Figure 12.41 Chemical evolution of lignite to coal. Hatcher and Clifford (1997). With permission from Elsevier.

resulting material is now called *bituminous coal*, which requires temperatures in the range of 40–100°C. Bituminous coal has a fairly bright appearance and contains 75% or more C and a water content less than 10%. At this point, vitrinite reflectance reaches 0.5%, and 70% or more the carbon is in aromatic.

With further heating, aromatization of cycloalkyl structures becomes the dominant process, releasing methane. Aromatization and loss of methane reduces the H/C ratio, which decreases rapidly upon further heating. In the temperature range of 100–150°C, *anthracite* is formed as the H/C ratio decreases below 0.5%. Anthracite is characterized by vitrinite reflectance of >2.5% and a carbon content of greater than 90%. Ninety percent or more of this carbon is in aromatic structures. As in kerogen, these aromatic structures initially take the form of randomly ordered nuclei. During the geochemical stage of coalification, these nuclei become increasingly ordered, so that by the anthracite stage, they are arranged as approximately parallel sheets, progressing toward the arrangement in graphite.

12.8 ISOTOPE COMPOSITION OF HYDROCARBONS

12.8.1 Bulk isotopic composition

The isotopic composition of sedimentary organic matter and its derivatives, such as coal and oil, depend on (1) the isotopic composition of the originally deposited organic matter and (2) isotopic fractionations occurring during diagenesis and subsequent thermal evolution. The ultimate source of carbon in sedimentary organic matter is atmospheric CO_2 or marine HCO_3^-. The $\delta^{13}C_{PDB}$ value of the former is about –7‰, while the $\delta^{13}C_{PDB}$ in average surface ocean water is +2.2‰ (both of which vary somewhat). As we found in Chapter 9, isotopic fractionation during photosynthesis results in organic carbon being substantially lighter (lower $\delta^{13}C$) that either atmospheric or dissolved CO_2. Terrestrial C_3 plants typically have $\delta^{13}C$ of –25 to –30‰, C_4 plants have $\delta^{13}C$ of –10 to –15‰, while marine plants are somewhat more variable in isotopic composition (–5 to –30‰), though on average they are perhaps heavier than terrestrial C_3 plants. There is some further fractionation of carbon isotopes as other organic molecules are synthesized, with lipids being isotopically lighter than carbohydrates and proteins. While these differences are small compared with the fractionation during photosynthesis, they do appear to persist through diagenesis.

Most living organisms have δD_{SMOW} in the range of –60 to –150‰. Within this range, hydrogen isotope ratios vary due to hydrogen isotope fractionation in the hydrologic cycle (Chapter 9). Terrestrial plants tend to be more deuterium-depleted than marine ones, and terrestrial plants from cold climates are particularly depleted. Lipids are depleted in δD relative to bulk organic matter by 60‰ or more. Most kerogen, coal, and oil show about the same range in δD as do organisms, but lipid-rich kerogen and oil can have substantially lower δD.

The situation with nitrogen isotopes is similar. Nitrogen isotope ratios in sedimentary organic matter generally reflect that of the biomass from which it is derived, with terrestrial plants having slightly lower average $\delta^{15}N_{ATM}$ than marine plankton (Fogel and Cifuentes, 1993). $\delta^{15}N$ generally decreases somewhat during diagenesis due to bacterial utilization of short chain peptides following peptide bond hydrolysis (Macko *et al*., 1993). In contrast, sulfur bound in organic matter is more likely to have been derived from inorganic forms of sulfur; in seawater this is ultimately sulfate, which in the modern ocean has $\delta^{34}S$ of +20. As we found in Chapter 9, there is typically a large negative fractionation during bacterial sulfate reduction; consequently, modern marine kerogen typically has a $\delta^{34}S$ of around –10. The exact values depend in part on the extent to which the system was open or closed during reduction, the latter case resulting in more limited fractionation. Sulfur isotope ratios are little affected by catagenesis and migration, and thus are sometimes used to correlate oils with their source rocks.

For the most part, isotopic fractionation of carbon during diagenesis of organic matter is small. As a result, the $\delta^{13}C$ of sedimentary organic matter is typically within a few per mil of the $\delta^{13}C$ of the biomass from which it is derived. Sedimentary organic matter and humic substances in soil and water tend to be slightly more depleted (by 2 to 3 per mil) in ^{13}C than the organisms from which they are

derived, though there are cases where the opposite has been observed. There are several possible causes for this (reviewed in Tissot and Welte, 1984; Hoefs, 1987; Macko *et al.*, 1993). First, functional groups, such as carboxyl, tend to be relatively ^{13}C rich. Loss of functional groups during diagenesis or condensation of humic substances will drive the residual organic carbon to lower $\delta^{13}C$. Second, there appears to be a kinetic fractionation involved in condensation of humic substances and kerogen-like molecules. Third, preferential remineralization of proteins and carbohydrates leaves a lipid-rich residue, which will be isotopically light.

Fractionation of carbon isotope ratios during thermal evolution through the oil generation stage drives kerogen toward higher $\delta^{13}C$ values, but the difference is small. In immature kerogen, bitumens are depleted in $\delta^{13}C$ compared with kerogen, but this difference decreases with increasing maturity (Schoell, 1984). Sofer (1984) found that $\delta^{13}C$ of the oils are within 2‰ of the isotopic composition of its source kerogen. Conkright and Sackett (1992) found that $\delta^{13}C$ of organic carbon in sediment cores from DSDP (Deep Sea Drilling Project) Site 368 near the Canary Islands increased with proximity to an intrusive diabase sill by 2–3‰. They attributed the decrease to thermal maturation and loss of isotopically light methane caused by heating from the sill.

There can be significant fractionation of carbon and hydrogen isotopes in the generation of methane. As Figure 12.42 shows, methane produced by methanogenic bacteria, called "biogenic methane", during diagenesis is highly depleted in ^{13}C. Methane produced during catagenesis, termed "thermogenic methane" is depleted in both ^{13}C and deuterium compared with associated oil and kerogen. These fractionations reflect the lower strength of ^{12}C–^{12}C bonds compared with ^{13}C–^{12}C bonds and therefore the greater ease with which the former are broken. As the metagenesis stage is entered, however, the isotope fractionation between methane and residual kerogen decreases and the isotopic composition of methane generated during this stage approaches that of kerogen. This is just what we would expect from both the inverse relationship between the fractionation factor and temperature and the decreasing fractionation as reactions proceed to completion (see Chapter 9).

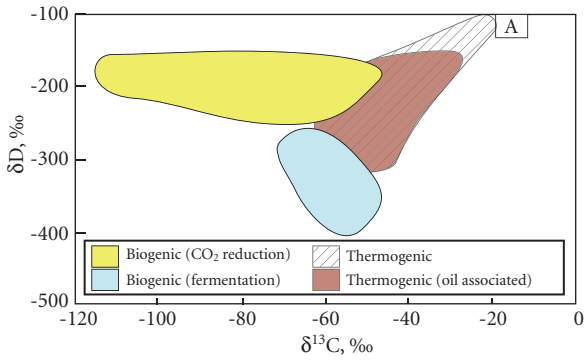

Figure 12.42 Isotopic composition of methane from various sources. "Biogenic" methane is methane produced by methanogens during diagenesis; "Oil Associated" is methane associated with oil; "A" is the composition of abiogenic methane from mid-ocean ridge hydrothermal systems. Modified from Schoell (1984) and Whiticar (1990). With permission from Elsevier.

Methane in mid-ocean ridge hydrothermal vent fluids (Figure 12.42) has systematically higher $\delta^{13}C$ (–15 to –20‰) than biogenic and thermogenic methane derived from sedimentary organic matter (Schanks *et al.*, 1995), demonstrating its abiogenic origin. The isotopic fractionation between methane and CO_2 in these fluids suggests equilibration at temperatures in the range of 600–800°C (Whelan and Craig, 1983).

12.8.2 Compound-specific isotopic analysis

Because the isotopic composition of oil is similar to that of its parent kerogen, isotope ratios are a widely used exploration tool in the petroleum industry. An isotope ratio for bulk organic matter is, however, a tool of rather limited usefulness. For example, bulk isotopic analysis cannot be used to discriminate between depositional environments, as the isotopic differences between marine and terrestrial organic matter are neither sufficiently large nor sufficiently systematic. A far more powerful tool emerges through isotopic analysis of specific compounds, particularly biomarkers. Compound specific isotopic

analysis has proved useful not only in petroleum exploration, but in environmental and paleontological research. For example, the carbon isotopic distinctions between C_3, C_4, and marine biomass (Figure 9.18) is retained in derivative n-alkanes in sedimentary matter. Based on isotopic analysis of C_{29} n-alkanes derived from leaf waxes in sediment cores from Central American lakes, Huang *et al.* (2001) showed that over the last 27,000 years, the ratio of C_4 to C_3 plants in the region depended on climate. As the last glacial period ended, conditions in the region became more arid, and the proportion of C_4 plant-derived alkanes increased. Isotopic compositions of specific components of petroleum gases (e.g., methane, ethane, propane) can be related to specific classes of kerogen and correlated to their source rocks (Killops and Killops, 2005).

Isotopic analysis of C_{37} alkadienone (i.e., a 37-carbon chain including a ketone bond and two unsaturated carbons) in marine sediments has proved to be useful in reconstructing variations in atmospheric CO_2. This molecule is a component of cell membranes of a specific group of haptophyte algae (e.g., coccolithophorids such as *Emiliania huxleyi*), and is particularly resistant to diagenetic change (indeed, it survives in petroleum). The idea behind this approach is that lower atmospheric CO_2 levels should result in greater isotopic fractionation between atmospheric CO_2 and organic matter produced by photosynthesis. This is true because isotopic fractionation during photosynthesis, Δ, depends on the extent to which intracellular CO_2 is fixed into organic matter (Section 9.5.1). When CO_2 is abundant, photosynthesis ^{12}C is selectively fixed and the fractionation is large. When CO_2 is less abundant, photosynthesis is less selective, proportionally more ^{13}C is fixed into organic matter, and the fractionation is smaller. Pagani *et al.* (1999) analyzed $\delta^{13}C$ in C_{37} alkadienone and in carbonate shells of planktonic foraminifera in Tertiary marine sediments, the latter being a measure of dissolved inorganic CO_2 (which, as we saw in Chapter 6, is primarily in the form of bicarbonate). Relating the difference between the two requires overcoming two complications. The first is that the fractionation will also depend on the photosynthesis rate: at high rates, there will be a drawdown of intracellular CO_2 and the fractionation will be small even if extracellular CO_2 is abundant. Pagani *et al.* (1999) essentially finessed this issue by focusing on sediments from areas of the ocean where photosynthesis is limited by nutrient abundance (oligotrophic regions); in other words, they assumed a constant photosynthesis rate. The second complication is that marine phytoplankton draw CO_2 from the ocean, not the atmosphere; so one final factor is the relationship between CO_2 in ocean surface waters. In oligotrophic open-ocean surface waters, this should depend only on the solubility of CO_2 in water, which depends, effectively, only on temperature. Combining paleotemperature estimates based on $\delta^{18}O$ (discussed in Chapter 9), and $[CO_2]_{aq}$ estimated from the fractionation between C_{37} alkadienone and carbonates in the same sediments, they estimated atmospheric CO_2 through most of the Miocene and late Oligocene (Figure 12.43). The results were surprising because they showed that CO_2 has been near its pre-industrial modern level throughout most of the Miocene. Thus the cooling that occurred in the late Miocene was not due to decreasing atmospheric CO_2 as was widely suspected. P_{CO_2} does appear to have declined sharply at the Oligocene–Miocene boundary, coinciding with a known

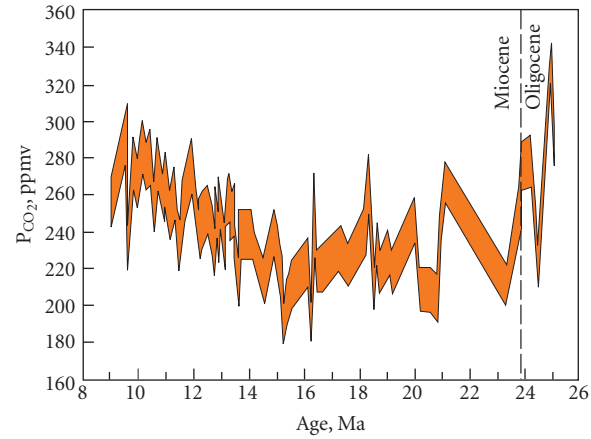

Figure 12.43 Atmospheric CO_2 concentration during the Miocene calculated from the difference between $\delta^{13}C$ in C_{37} diunsaturated alkenones and carbonate in sediments from DSDP site 588 by Pagani *et al.* (1999). Reproduced with permission from the American Geophysical Union. The red area falls between maximum and minimum values calculated using different assumptions.

glacial event, but otherwise there is little relationship with apparent climate change over this period. There is generally good agreement between this method of estimating atmospheric CO_2 concentrations and estimates based on boron isotopic measurements in foraminiferal shells discussed in Chapter 9.

12.9 THE CARBON CYCLE AND CLIMATE

In 1896, building on the 1824 work of Joseph Fourier, Svante Arrhenius (whom we met in Chapter 5 in connection with his contribution to kinetic theory) published a paper entitled "On the influence of carbonic acid in the air upon the temperature of the ground" in which he suggested that the concentration of atmospheric CO_2 might be increasing as a result of the extensive burning of coal that began with the industrial revolution. Taking note of the way in which CO_2 absorbs infrared radiation, he supposed that increasing atmospheric CO_2 concentration would result in warming of the Earth's surface temperature. Arrhenius thus provided the first warning that burning of fossil fuels would result in greenhouse-driven climate change, as well as the key to understanding how climate has evolved over the entirety of Earth's history. In this final section, we will have space only to briefly review greenhouse climate theory and carbon geochemistry. There are of course, many books that cover this topic in much greater depth.

12.9.1 Greenhouse energy balance

A greenhouse remains warm because visible light from the Sun is readily transmitted through glass. The energy is adsorbed by the ground and objects within the greenhouse and is converted to thermal motion of atoms and molecules: heat. As a consequence of that heat, the atoms radiate electromagnetic radiation. The wavelength emitted by those atoms is in the infrared in accordance with Wein's Law, which states that the wavelength of maximum spectral emittance of black body radiation is inversely related to temperature. Glass, however, absorbs much of that infrared radiation rather than transmitting it. The glass then re-emits radiation, about half of which is directed downward back into the greenhouse. This effectively traps energy in the greenhouse and it warms. As it does, it emits radiation more intensely (according to Stephan's Law, the intensity of black body radiation is proportional to the fourth power of temperature) until an equilibrium sets in such that as much radiative energy escapes the greenhouse as arrives from Sun.

The Earth's atmosphere works in much the same way. Visible light from the Sun is largely passed through the atmosphere and is adsorbed by the Earth's surface, which then radiates in the infrared. That radiation is adsorbed when its frequency matches a resonance of the vibrational frequency of the bonds in a particular molecule. The principal gases in the modern Earth's atmosphere, N_2, O_2, and Ar, are monatomic or symmetric diatomic molecules that do not absorb in the infrared part of the spectrum. However, certain trace gases in the atmosphere, notably H_2O, CO_2, CH_4, and N_2O, strongly absorb certain wavelengths of infrared radiation. CO_2, CH_4, and N_2O absorb at different frequencies and thus each independently affects the atmospheric energy balance. However, the absorption bands of H_2O and CO_2 do overlap somewhat. Because relatively small amounts of these gases can absorb a large fraction of the radiation at specific frequencies, the effect of these gases on atmospheric energy balance does not scale linearly with their concentrations, but rather with the log of their concentrations. Thus, for example, small changes in the abundance of CH_4 have a much greater effect on the energy balance than do small changes in more abundant CO_2, even though CO_2 absorbs at frequencies close to the Earth's maximum spectral emittance and is thus inherently a more effective greenhouse gas than CH_4, which adsorbs on the edge of the Earth's spectrum.

The combined effect of these gases is to absorb much of the infrared radiated by the Earth's surface and to raise the average temperature of the Earth's surface from 254 K (−19°C) to 286 K (+13°C). H_2O is the most powerful of the greenhouse gases, because it absorbs over a relatively wide range of frequencies and because its concentration is relatively high (its atmospheric concentration can be up to 4% on a very hot, humid day). However, the residence time of water in the atmosphere is quite short, so that its effect alone can only be limited. Its concentration in the atmosphere is strongly related to

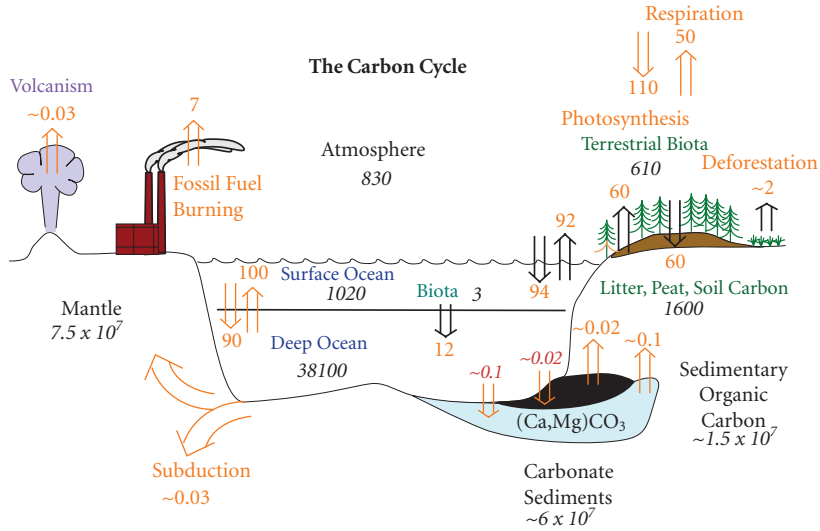

Figure 12.44 The carbon cycle. Numbers in italic show the amount of carbon (in 10^{15} grams or gigatons, Gt) in the atmosphere, oceans, terrestrial biosphere, and soil (including litter, debris, and so on). Fluxes (red) between these reservoirs (arrows) are in Gt/yr. Magnitudes of reservoirs and fluxes are principally from Siegenthaler and Sarmiento (1993) and Falkowski *et al.* (2000).

temperature and at 254 K, the atmosphere would contain very little water indeed. Water thus merely amplifies the effect of the primary greenhouses gases, CO_2, CH_4, and N_2O: warmer temperatures lead to more evaporation and more humid air and a stronger greenhouse effect which leads to warmer temperatures, and so on. Variations in atmospheric H_2O are important in short-term, local variations in temperature (this is why, for example, nights in humid regions are warm and nights in arid ones are cold). On long time-scales, however, variations in the concentration of CO_2 and the other greenhouse gases control climate. Variations in atmospheric greenhouse gas concentrations are a result of how carbon is cycled between the atmosphere and other reservoirs and how the Earth and life have evolved over the last 4.5 Ga. We consider these in the following sections.

12.9.2 The exogenous carbon cycle

We will adopt (and anglify) the French word "*exogène*" to refer to the Earth's surface, including the atmosphere, biosphere, hydrosphere, cryosphere, soil, weathering crystalline rock, and reactive, unlithified sediments. Carbon in the exogene cycles between a variety of forms, of which organic carbon is one. This carbon cycle is illustrated in Figure 12.44. Roughly 110 gigatons (Gt) of carbon are fixed into organic carbon by photosynthesis of terrestrial plants every year. About half of this, around 50 Gt, is quickly returned to the atmosphere through respiration of plants or animals feeding on them, while the other half flows into a reservoir of non-living organic carbon that includes leaf litter, dead trees, peat, and soil organic matter. The mass of this reservoir is approximately steady-state, so that roughly this same amount is oxidized to CO_2 every year. The non-living organic carbon reservoir contains more than twice as much carbon as the terrestrial biota (more than 99% of which is plants), and more carbon than is present in the atmosphere and biota combined. Atmospheric CO_2 also readily exchanges with dissolved forms of carbon in the ocean, with roughly 90 Gt of CO_2 dissolving in the ocean and a similar amount exsolving out every year. The marine dissolved carbon reservoir, about 98% of which is HCO_3^-, contains roughly 50 times as much carbon as does the atmosphere. Carbon is cycled far more rapidly between organic and inorganic forms in the marine environment: net primary production (photosynthesis minus respiration) of marine phytoplankton is

roughly 40 Gt, about 80% of terrestrial net primary production, even though the marine biosphere is 200 times smaller than the terrestrial one. Only the surface layer of the ocean, roughly the upper 200 m, exchanges readily with the atmosphere. The deep ocean, which contains the bulk of the dissolved carbon, is isolated from the atmosphere. Carbon flows into that reservoir either through downwelling of surface waters, which occurs mostly near the poles, or through falling organic remains such as dead organisms and fecal pellets. Nearly all of that falling organic matter is remineralized to HCO_3^- before reaching the sediment. The process by which carbon moves from the atmosphere into the marine biota via photosynthesis and from there into the deep ocean through sinking organic particles and then into dissolved CO_2 is known as the *biologic pump*. In addition, carbonate shells of planktonic organisms, most notably coccolithophorids and foraminifera, also fall through the water column to the deep water. Those shells falling below about 4000 m largely redissolve because water at this depth becomes strongly corrosive to calcite. One reason it is corrosive is that its pH is lower. As a consequence, dissolved CO_2 concentrations are significantly higher in the deep ocean than in surface waters. This deep-water CO_2 eventually returns to the surface through upwelling and mixing, but the process is slow. The average ventilation time of the ocean (i.e., the average time deep water spends out of contact with the atmosphere) is about 1500 years based on ^{14}C analysis. Thus the biologic pump acts to sequester CO_2 from the atmosphere and maintains atmospheric CO_2 levels some 150 to 200 ppm lower than it would be otherwise (Falkowski *et al.*, 2000).

On short geologic time-scales, 100,000 years and less, atmospheric CO_2 levels are controlled by the balance of carbon fluxes into and out of the oceans and the terrestrial biosphere and soils. Over the last million years or so, these fluxes have varied in response to glacial cycles driven by Milankovitch forcing (Chapter 9), resulting in variation in atmospheric CO_2 concentrations. As Figure 12.45 shows, CO_2 varied from around 190 ppm in glacial episodes to around 280 ppm in interglacial episodes.

Glacial cycles affect CO_2 fluxes in a number of ways. The first of these is volume and temperature of the oceans. The smaller the volume of the ocean, the less CO_2 it can hold; ocean volume over the past million years or so has been controlled by waxing and waning of ice sheets. CO_2 is more soluble in water at lower temperature, so low temperatures favor a net flux of CO_2 from the atmosphere to the oceans. The effect of glacial cycles on these

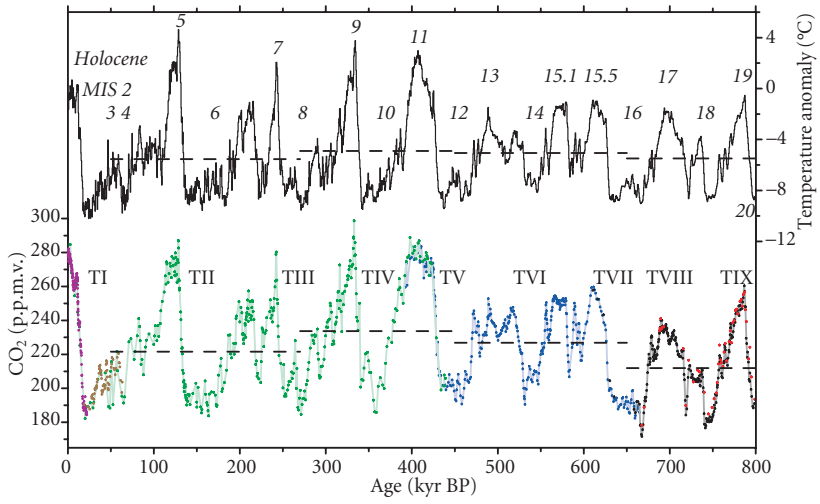

Figure 12.45 Comparison of CO_2 in bubbles (gray shows analytical uncertainties) in the EPICA ice core with temperatures calculated from δD. Reprinted by permission from McMillan Publishers Ltd: From Luthi *et al.* (2008). Numbers on the temperature plot are marine isotope stages. T_I, T_{II}, etc., on the CO_2 plot are terminations of glaciations.

two factors is thus opposite. Glacial cycles also affect the terrestrial biota, but, again, with opposing effects. During glacial times, sea-level drops and the area available for terrestrial vegetation expands, but expansion of glaciers also reduces this area. Precipitation patterns also change from glacial to interglacial times and also affect the biota as the total area of arid regions changes. Variations in climate and the terrestrial biota in turn drive variations in the mass of carbon stored as dead organic matter in soils, forest litter and peat. Interestingly, there is no simple relationship between the mass of living carbon in a biome and the mass of dead carbon stored in soils. For example, two biomes, tundra and grassland, account for only 4% of the terrestrial biomass yet account for more than a quarter of organic matter stored in soils. This is because organic matter decays slowly in these environments, whereas it decays quite quickly in tropical and temperate forests, which together account for over 60% of the terrestrial biomass. Thus the interaction between climate, atmospheric CO_2, and the terrestrial biomass is complex and is has not yet been fully quantified.

The most important changes in CO_2 fluxes into and out of the atmosphere in glacial–interglacial cycles appear to be those into and out of the oceans. These fluxes change in response to climate-driven changes in ocean circulation, which change the ventilation time of the ocean and hence the storage of CO_2 in the deep ocean. Toggweiler *et al.* (2006) suggested that the key ocean circulation changes result from a climate-driven migration of the westerly winds in the Southern Ocean. In the present interglacial climate, the most intense westerly winds are located south of the Antarctic polar front. As a result of a phenomenon called Ekman transport, these winds drive water away from Antarctica, and as a result, water rises, or "upwells" from depth, allowing CO_2 build-up in the deep ocean to vent to the atmosphere, keeping atmospheric CO_2 concentrations high. During glacial times, these westerlies shifted equatorward allowing for build-up of CO_2 in circum-Antarctic deep water. In addition, changes in the efficiency of the biologic pump can affect the balance of CO_2 between ocean and atmosphere (e.g., Boyle, 1988). Most of the ocean is oligotrophic, meaning that photosynthesis is limited by the abundance of nutrients in the surface water. Hence, the rate at which the biologic pump works is governed by surface-water nutrient levels. These are in turn governed by factors such as the rate at which nutrients are delivered from the land, the areal extent of continental shelves where nutrients can be recycled from the ocean bottom, and return of nutrient-rich deep water to the surface by ocean circulation. Since CO_2 is a strong greenhouse gas, this shift of CO_2 between the atmosphere and the ocean serves to amplify the climate changes that produce them in the first place. In this way, the quite small changes in geographic and temporal distribution of insolation were strengthened sufficiently to produce the remarkable glacial–interglacial cycles of the Pleistocene.

12.9.3 The deep carbon cycle

Carbon at the Earth's surface is also part of a deeper, slower cycle. A small fraction of the organic carbon fixed every year is buried in sediments (Figure 12.44). Much of what is initially buried in sediment is remineralized during diagenesis, but a fraction is sequestered from the exogene for long geologic times. Some fraction of this sedimentary organic carbon eventually returns to the exogene through weathering, and some fraction is subducted into the mantle. Some of the subducted organic carbon is returned relatively quickly to the atmosphere through subduction-related volcanism or decarbonation during metamorphism, while some continues into the deep mantle. That too can eventually return to the atmosphere through mid-ocean ridge and mantle plume-related volcanism.

When dissolved in water, CO_2 forms carbonic acid and dissociates (Chapter 6), providing hydrogen ions that then attack silicate minerals:

$$CO_2 + H_2O \rightleftharpoons H^+ + HCO_3^-$$

$$2H^+ + H_2O + CaAl_2Si_2O_8 \rightleftharpoons Al_2Si_2O_5(OH)_4 + Ca^{2+}$$

Calcium released in this way is carried by rivers to the sea along with bicarbonate ions where they precipitate as calcite:

$$Ca^{2+} + HCO_3^- \rightleftharpoons H^+ + CaCO_3$$

Much of the calcite redissolves in the deep water or sediment, but some is buried as part of the carbonate reservoir in Figure 12.44. The effect of silicate weathering is thus to remove CO_2 from the atmosphere. Weathering of limestone has no effect on atmospheric CO_2, however, as carbonate ions produced in the process are also precipitated as calcite in the ocean and thus carbonate is recycled back into the sedimentary carbonate reservoir. As is the case with sedimentary organic carbon, sedimentary carbonate can eventually return to the atmosphere through metamorphism or volcanism.

Together, the relative rates of volcanism and metamorphism, weathering of sedimentary organic matter, weathering of silicates (and resulting burial of sedimentary carbonate), and burial of sedimentary organic matter control the amount of carbon in the oceans, atmosphere, and biosphere on long geologic time-scales (more than about 1 Ma), as first noted by Berner *et al.* (1983). For the last few hundred million years, the masses of carbon in the various reservoirs illustrated in Figure 12.44 have been approximately constant and the fluxes into and out of the exogene have been more or less at steady-state. The modifier "more or less" is important. Indeed, the GEOCARB model developed by R.A. Berner and his colleagues at Yale University over the years (e.g., Berner *et al.*, 1983; Berner, 2006) begins with an assumption of steady-state and then uses carbon isotope variations in marine sediments as primary input to model variations in atmospheric CO_2 that result from imbalances in fluxes into and out of the exogene, that is, deviations from steady-state. Small changes in these fluxes likely account, at least in part, for the climatic extremes that have occurred in the Phanerozoic. The Pleistocene glaciations are only the most recent example; glaciations also occurred at the end of the Ordovician and from the late Carboniferous into the Permian. In between these times, the Earth experienced warm periods, such as the Cretaceous, when the poles were ice-free and the oceans circulated in a far different manner than they do today.

The fluxes into and out of the exogene do not operate independently but are coupled in complex ways that result in both positive and negative feedbacks, just as is the case in the exogenous carbon cycle. These are illustrated

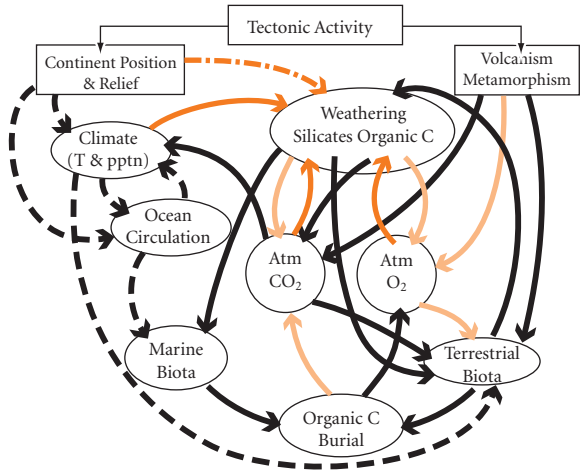

Figure 12.46 Feedback loops in the long-term carbon cycle. Black arrows represent positive feedbacks, gray arrows represent negative feedbacks, and dashed arrows are complex feedbacks (can be positive or negative). After Berner (1999) and Killops and Killops (2005).

in Figure 12.46. Just as in the exogenous cycle, these feedbacks are linked to and affect climate. In the exogenic carbon cycle, Milankovitch cycles drove variations in the system through the Pleistocene. In the deep carbon cycle, the principal external factor is tectonic activity, including continental position, uplift, volcanism, and metamorphism. Continent position and uplift directly affect global climate, but in both positive and negative ways (climate is "positive" in this scheme when it is warm and wet). Continent position and climate can both also affect ocean circulation, albeit in complex ways, which affects nutrient distribution; that, in turn, affects the marine biota and the biologic pump. Volcanism, which is closely linked to tectonic activity, affects the terrestrial biota directly by supplying soil nutrients and emitting CO_2 and reduced gases to the atmosphere (the latter consuming O_2). Uplift increases erosion and weathering, which supplies nutrients to both the terrestrial and marine biota. Increasing terrestrial and marine bioproductivity results in more burial of organic matter in sediments, which draws down atmospheric CO_2 and increases atmospheric O_2. Increasing atmospheric O_2 increases weathering of sedimentary organic carbon, while increasing CO_2,

along with organic acids produced by the terrestrial biota, increases silicate weathering. O_2 affects the biota through wildfires: fires are more likely and burn more extensively at higher O_2 levels. Increased silicate weathering decreases atmospheric CO_2, which decreases global temperature, which decreases weathering. Climate also affects the terrestrial biota, albeit in complex ways. These complex interactions have led to variations in climate through the Phanerozoic, such as the Ordovician, Permo-Carboniferous, and Pleistocene glaciations.

12.9.4 Evolutionary changes affecting the carbon cycle

Superimposed on the interactions illustrated in Figure 12.46 have been three long-term unidirectional changes that have affected the Earth, the carbon cycle, and climate.

- The first of these has been a steady increase in brightness of the Sun and, consequently, insolation. Stars grow progressively brighter over their main sequence (Figure 10.1) lifetimes. The Sun is now about 30% brighter than it was 4.5 billion years ago when it first became a main sequence star. This increase in insolation would result in a surface temperature increase of nearly 22°C, all other factors being equal. Interestingly, the present mean global surface temperature is now about 13°C. This implies a mean surface temperature on the young Earth of –9°C, well below freezing, all other things being equal. Yet, liquid water appears to have been present on Earth nearly continuously since 3.8 Ga. This conundrum is known as the *faint young Sun paradox*.
- The second change is a decline in tectonic activity. Energy to drive tectonic activity comes from two sources: radioactive decay of U, Th, and K, and initial heat. The activity of these radionuclides has, of course, decreased exponentially over time. Based on the estimated abundance of radionuclides in the Earth (Table 11.3), radioactivity accounts for less than half the present heat loss from the Earth (about 45 terawatts); the remainder must reflect long-term cooling of the Earth from an initially hotter state. This long-term loss of heat and decline in radioactivity must necessarily result in long-term decline in tectonic activity, albeit not necessarily a steady one.
- The third change has been the evolution of life, which has had a profound effect on the nature of the atmosphere, and, as a result, on climate. The Earth's atmosphere in Hadean and early Archean times would have certainly been much different from the present one. Oxygen would have been absent; instead CO_2 would likely have been the dominant component, as it is in the atmospheres of Mars and Venus. It may well have been modestly reducing, with some CH_4 present. It is unclear when life, and photosynthetic life in particular, first arose, but a case can be made that oxygenetic photosynthetic life was present on Earth by 3.5 billion years ago, and it was almost certainly present by 2.7 Ga, based on cyanobacteria-derived biomarkers (methyl-hopanoids) in sediments of that age. Since then, photosynthesis has converted atmospheric CO_2 to organic matter, producing O_2 as a byproduct. Most of the organic matter produced by photosynthesis has simply recycled back into CO_2 through respiration, consuming the O_2 originally produced. However, some of that organic matter has been buried in sediment, leading to a drawdown of atmospheric CO_2 and build-up of O_2. Indeed, there is more than three times as much organic carbon in sediments as needed to account for the O_2 in the atmosphere (this implies large amounts of O_2 have been consumed by oxidizing sulfur and iron). The drawdown of CO_2, and possibly methane as well, in the atmosphere has in turn affected climate. Indeed, a decrease in greenhouse gas abundances over geologic history appears to be the only way to resolve the "faint young Sun paradox" mentioned above: higher concentrations of atmospheric CO_2 and CH_4 provided a stronger greenhouse effect, keeping average surface temperatures above freezing throughout nearly all of the Precambrian. If the greenhouse effect is provided only by CO_2 (as opposed to CO_2 and CH_4), the amounts needed to offset the dimmer Sun would be considerable: at the beginning of the Proterozoic (2.5

billion years ago), 100 times the present atmospheric levels of CO_2 would have been needed just to keep the average surface temperature above freezing. Lower concentrations would have been needed if substantial methane were present. At the beginning of the Phanerozoic when the Sun was only 5% dimmer than at present, a CO_2 concentration some ten times the present one would have been needed to maintain an average surface temperature similar to the modern one (assuming CH_4 concentrations similar to modern ones). While photosynthetic life was present in the oceans in Archean times, it was not until the Paleozoic that land plants evolved. The evolution of terrestrial flora provided a new environment in which organic matter could be buried, namely bogs, swamps, and mires, and ultimately converted to coal. Vast deposits of coal produced during the aptly named Carboniferous period testify to the effect of the new terrestrial biota on the carbon cycle. In addition, the invasion of the land by plants accelerated silicate weathering by releasing organic acids from roots. Finally, the evolution of terrestrial flora would have changed climate directly by changing the Earth's albedo (reflectivity). Deserts, sand, and soil, presumably the Precambrian land cover, reflect 25–30% of solar radiation back into space. Forests reflect only about 10% of that radiation. Thus the decrease in albedo in the Paleozoic that would have resulted from the evolution of terrestrial flora would have effectively increased insolation and had a warming effect on climate.

12.9.5 The carbon cycle and climate through time

Figure 12.47 shows Berner's (2006) modeled atmospheric CO_2 concentrations over the Phanerozoic. The model is based on the relationships illustrated in Figure 12.46 and the record of carbon isotope ratios in marine carbonate sediments. The latter change in response to shifts in the fluxes shown in Figure 12.46. For example, because organic carbon has low $\delta^{13}C$, an increased burial of organic carbon drives the isotopic composition of carbon in the exogene toward more positive

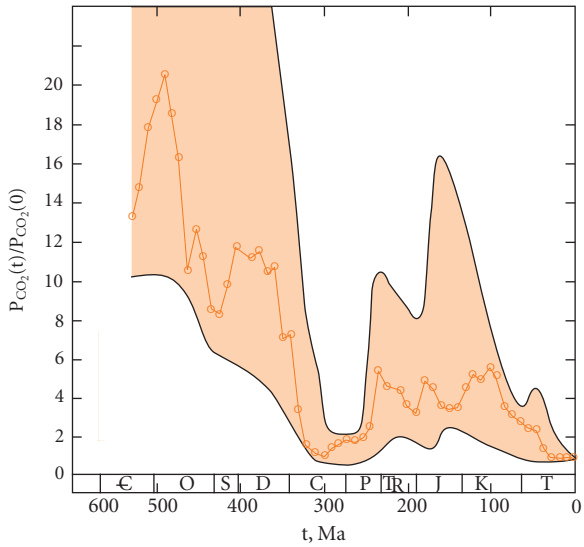

Figure 12.47 Concentration of atmospheric carbon dioxide over the Phanerozoic. Open red circles show the modeled values of Berner (2006). Uncertainty in the model are shown as the shaded area and are taken from Berner and Kothavala (2001).

values. Increased weathering of organic carbon would have the opposite effect. These isotopic shifts are reflected in the isotopic composition of carbonates precipitated from the oceans. The overall picture suggested by this model is one of declining atmospheric CO_2, but if the model is correct, the decline has not been steady. A decline through the Ordovician led to a glacial epoch in the Late Ordovician–Early Silurian. The Berner model suggests this was due to weathering of silicate rock (specifically volcanics). Continental position likely also played a role, as most evidence of glaciation comes from areas positioned near the South Pole at the time. CO_2 recovered in the Silurian, but declined again in the Devonian and Carboniferous, leading to the Permo-Carboniferous glaciation. This time the cause appears to be burial of vast amounts of organic carbon in bogs, swamps, and mires that was ultimately transformed into coal. Atmospheric CO_2 recovered in the Mesozoic, but not to levels seen in the Paleozoic (remember, however, that less CO_2 was needed to maintain the same temperature). After reaching concentrations perhaps 5 times greater than present ones, atmospheric CO_2 declined

in the late Cretaceous and early Tertiary periods. An essentially similar decline over this period is seen in the model of Hansen and Wallmann (2003). Judging from CO_2 levels deduced from diunsaturated alkenones (Figure 12.43) and boron isotopes (Figure 9.47), long-term atmospheric CO_2 levels have remained low throughout the late Tertiary (the Neogene) into the Quaternary, although shorter term variations have occurred as a result of perturbations of the exogenous carbon cycle driven by Milkankovitch cycling (Figure 12.45).

Knowing how atmospheric CO_2 and climate varied in the Precambrian is a much more difficult proposition. There is some sparse and equivocal evidence for glaciation in the late Archean, around 2.8 Ga, and strong evidence of glaciations in the Paleoproterozoic (occurring roughly between 2.4 to 2.2 Ga) and in the Neoproterozoic (occurring roughly between 0.8 to 0.6 Ga). In both the Proterozoic events, glacial sediments (diamictites) appear to have been deposited at tropical, rather than polar, latitudes, based on paleomagnetic inclinations and other geologic indicators. Other evidence, such as the presence of marine sediments above and below them, indicate that they were deposited at low elevation. Examples of glacial sediments from the Neoproterozoic are found on every continent except Antarctica. These observations suggest that these glaciations were far more severe than Phanerozoic glaciations that followed (in the Pleistocene glaciations, for example, ice sheets reached no further south than about 40°N, although mountain glaciers were, and still are, present at lower latitudes). This has given rise to the "snowball Earth" hypothesis: glacial events so severe that oceans were entirely frozen over or nearly so (Kirschvink, 1992; Hoffman *et al.*, 1998). The record of the Paleoproterozoic glaciation is more equivocal, but low-latitude paleomagnetic inclinations in sequences in both North America and South Africa suggest the possibility that this too may have been a severe snowball-Earth-like glaciation that extended to the tropics.

The Paleoproterozoic diamictites in the Huronian formation in Canada occur stratigraphically above an older conglomerate containing abundant detrital pyrite (FeS_2) and uraninite (UO_2). That reduced minerals could survive erosion, transport, and deposition suggests they were deposited in an oxygen-free atmosphere. Other examples of detrital pyrite and uraninite in Archean-age sediments are relatively common, but with rare exceptions they do not occur in sediments younger than 2.2 Ga. The Huronian diamictites are overlain by redbeds: sandstones consisting of quartz coated with hematite. The hematite is indicative of an oxidizing atmosphere. Redbeds are absent in sediments older than 2.4 Ga, but occur more or less throughout the subsequent geologic record. Detrital pyrite and uraninite and redbeds are part of a suite of evidence, including mass-independent sulfur isotope fractionation discussed in Chapter 9 (Section 9.7.3), that significant amounts of atmospheric O_2 first appeared between 2.4 and 2.2 Ga. This period is known as the Great Oxidation Event (GOE). Oxygen levels in the atmosphere before the GOE were likely a factor of 10^{-5} lower than present and rose to 8–15% of present atmospheric levels during the GOE (e.g., Canfield, 2005; Holland, 2006). Thus the Paleoproterozoic Huronian glaciation corresponds closely in time with the appearance of atmospheric oxygen and this has led some scientists to suggest the two are related. Kasting and Ono (2006) suggested that the rise in atmospheric oxygen caused a drop in atmospheric CH_4 (a greenhouse gas). A drop in concentration of the latter from 10^{-3} to 10^{-5} would have produced a temperature decrease of 20°C, enough to trigger glaciation unless the early Proterozoic climate was much warmer than today. Alternative explanations involve pulses of mantle plume volcanism or rift-related volcanism (Melezhik, 2006; Eyles, 2008) that resulted in an increase in silicate weathering and drawdown of atmospheric CO_2.

Why did the atmosphere remain oxygen-free throughout the Archean and then rapidly increase in the Paleoproterozoic, when various lines of evidence suggest oxygenic photosynthesis began at least by 2.7 Ga and possibly much earlier? One reason is that iron and sulfur in the exogene would have been in reduced states. Before oxygen could build up in the atmosphere, the stock of reduced iron and sulfur would have to be substantially exhausted. Indeed, the observation that post-GOE Proterozoic paleosols, like modern ones, are iron-rich (because Fe^{3+} is insoluble and cannot be leached from them) while Archean

paleosols are iron-poor (because Fe^{2+} was leached) is evidence that considerable oxygen was consumed in the process of oxidizing soil Fe. Similarly, gypsum-bearing evaporites first appearing in the geologic record around the time of the GOE is evidence that oxygen was consumed in oxidizing sulfur to sulfate. Only after the stock of reduced Fe and S were oxidized could atmospheric O_2 rise. This would have taken time; just how long would have depended on the rate of oxygen production as well as the supply of reduced components to the surface by volcanism. Large variations in $\delta^{13}C$ in marine carbonates deposited around this time, including excursions to values as negative as –12‰, suggest disturbances to the exogenic carbon cycle which in turn support the possibility of changes in atmospheric greenhouse gas levels. Alternatively, Kump *et al*. (2001) and Holland (2009), among others, have suggested that a change in the composition of volcanic gases would account for the timing of the GEO. Although they differ in detail, both models conjecture that the mantle, and consequently volcanic gases, became more oxidizing through time as a result of subduction. Thus at least in some hypotheses both the GEO and the associated Paleoproterozoic glaciations resulted from processes and changes occurring deep within the Earth as well as changes occurring at the surface.

The geologic record of the Neoproterozoic glaciations is more complete, and there is compelling evidence that at least two of the glaciations, the Sturtian at around 715 Ma and the Marinoan at around 635 Ma, were severe and extended into the tropics. Although there is not yet complete agreement on this point, a consensus appears to be forming that not only were the continents largely ice-covered, but most or all of the ocean was frozen over by a thick layer of ice: a "snowball Earth". Indeed, the evidence of extensive glaciation is compelling enough that this period of the Neoproterozoic has been named the *Cryogenian*. In both cases, glacial sediments are overlain by thick deposits of marine carbonates, termed "cap carbonates" and are preceded by large negative $\delta^{13}C$ anomalies that return to positive values just before the glaciation. A possible earlier Kaigas glaciation at around 740 Ma and a later Gaskers glaciation at around 582 Ma appear to have been less severe.

The Cryogenian glaciations followed the break-up of the Rodinia supercontinent, which began around 800 Ma. Paleomagnetic reconstructions suggest that Rodinia was located at low latitude at the time and that the break-up proceeded longitudinally, so that the fragments remained at low latitude (in contrast to the break-up of Pangaea). Because of its size, interior regions of Rodinia would have been starved of ocean-derived moisture and weathering rates would have been slow. Weathering rates would have increased as it broke up and moisture reached its former interior. There is reason to think that extensive volcanism was associated with the continental rifting (as with Pangaea), and some evidence to support that thinking. At least until the beginning of the Cryogenian, atmospheric oxygen levels were likely as low as they had been throughout the Proterozoic – less than 18% of present levels. The oceans, particularly the deep oceans, were likely oxygen-poor, which may have allowed a much larger flux of CH_4 to the atmosphere. This methane would have played an important role in keeping the Earth's surface warm despite a dimmer Sun at the time.

These observations play key roles in models attempting to explain the initiation of glaciation. All models involve significant disturbances to the carbon cycle and a consequent crash in greenhouse gas inventory; beyond that they differ. Godderis *et al*. (2011) divided the models into three scenarios. In the first, Pavlov *et al*. (2003) suggested that rising oxygen levels around this time greatly reduced the methane flux from oxygen-poor oceans. That in turn reduced the CO_2 levels in the atmosphere (because the methane eventually oxidizes to CO_2). Schrag *et al*. (2002) proposed that the high rates of tropical weathering as Rodinia broke up led to enhanced ocean nutrient levels and productivity, and efficient burial of organic carbon. In the oxygen-poor ocean, however, much of this organic carbon would have been converted to methane and frozen into methane clathrate on continental margins. In their model, the methane clathrate eventually became unstable, flooding the atmosphere with CH_4, which soon oxidized to CO_2 (this accounts for the negative $\delta^{13}C$ in marine carbonates prior to glaciation). With the continents in the tropics, this CO_2 was quickly consumed by silicate

weathering, triggering a crash in the greenhouse gases. The model of Donnadieu *et al.* (2004) was similar in many respects, but called upon volcanic outgassing to provide an initial pulse of CO_2, which, as in the Schrag *et al.* (2002) model, is consumed by silicate weathering, which is greatly enhanced in the Donnadieu model by large amounts of young basalt exposed in the tropics. In all the models, once glaciation begins, the Earth "whitens" and the much greater albedo provides a powerful feedback driving further cooling.

The path out of the snowball state is less controversial. With the planet completely frozen, silicate weathering stops, yet volcanism continues. Over millions of year, sufficient CO_2 builds up in the atmosphere to warm the planet so that melting begins, and decreasing albedo then provides a feedback to drive further warming. In addition, there would have been almost no removal of atmospheric CO_2 by photosynthesis during the snowball phase, aiding its build-up in the atmosphere. The massive amounts of CO_2 in the atmosphere immediately after deglaciation produce a hothouse climate that greatly accelerates silicate weathering. The consequent flux of Ca^{2+}, Mg^{2+}, and HCO_3^+ to the ocean leads to massive carbonate precipitation, accounting for the cap carbonate sequences. Increases in $^{87}Sr/^{86}Sr$ in the Cryogenian are consistent with an enhanced flux of weathering products of the continents to the oceans, and hence are consistent with this aspect of the models.

The simple observation that photosynthesis survived the snowball Earth represents a problem for the most extreme versions of the hypothesis. If continents and oceans were thickly frozen, photosynthetic life could not have survived. One possible solution is that the oceans were not completely frozen, but climate simulations suggest that a nearly frozen Earth with open tropical seas is not stable – the oceans either freeze completely or begin to unfreeze. Another possible solution is that ice in the tropics was thin enough for sunlight to sustain at least some photosynthesis in the water below.

The termination of the Marinoan glaciation marks the beginning of the last period of the Proterozoic: the Ediacaran. Although one more, less severe, glaciation occurred in the Ediacaran, climate appears to have again stabilized. It was during the Ediacaran period that multicellular animals appeared (although sponge-like fossils from the Cryogenian have now been identified). Many scientists suspect the Cryogenian glaciations set the stage for Nature's experiments with multicellular animals in the Ediacaran and the explosion of life that saw the appearance of all animal phyla in the following Cambrian period.

12.9.6 Fossil fuels and anthropogenic climate change

Two hundred and fifty years ago humans began to replace traditional energy sources – muscle power, animal power, wind, and water – with a new energy source, coal. The coal-fired steam engine, first developed by James Watt to pump water from (ironically enough) a coal mine, was soon adapted to saw wood and cut stone, mill flour, spin yarn and weave fabric, provide transport, dig canals, and so on. Beginning in the mid-19th century, petroleum and natural gas began to supplement and partly replace coal and coal gas. The primary combustion product of all of these is, of course, CO_2. In 1896, Svante Arrhenius wrote the paper mentioned earlier, predicting that burning of fossil fuels should lead to an increase in atmospheric CO_2 concentration, which should in turn enhance the greenhouse effect and increase global temperatures. Arrhenius thought this was a good thing because it might prevent the Earth from entering another ice age and it should enhance agricultural productivity and help to feed a growing global population. At the time, there were no systematic measurements of atmospheric CO_2 concentration and global temperature record-keeping was just beginning, so the theory could not be tested.

Arrhenius's theory was largely ignored by the scientific community until the 1950s, when Hans Suess took notice of it. Suess was a nuclear chemist working on ^{14}C dating and concerned about an apparent decrease in the specific activity* of ^{14}C in the atmosphere. He suspected that increasing atmospheric CO_2 derived from fossil fuel, which would have a

* Recall from Chapter 8 that the specific activity is defined as the activity (decays per unit time) of ^{14}C divided by the amount of C in grams.

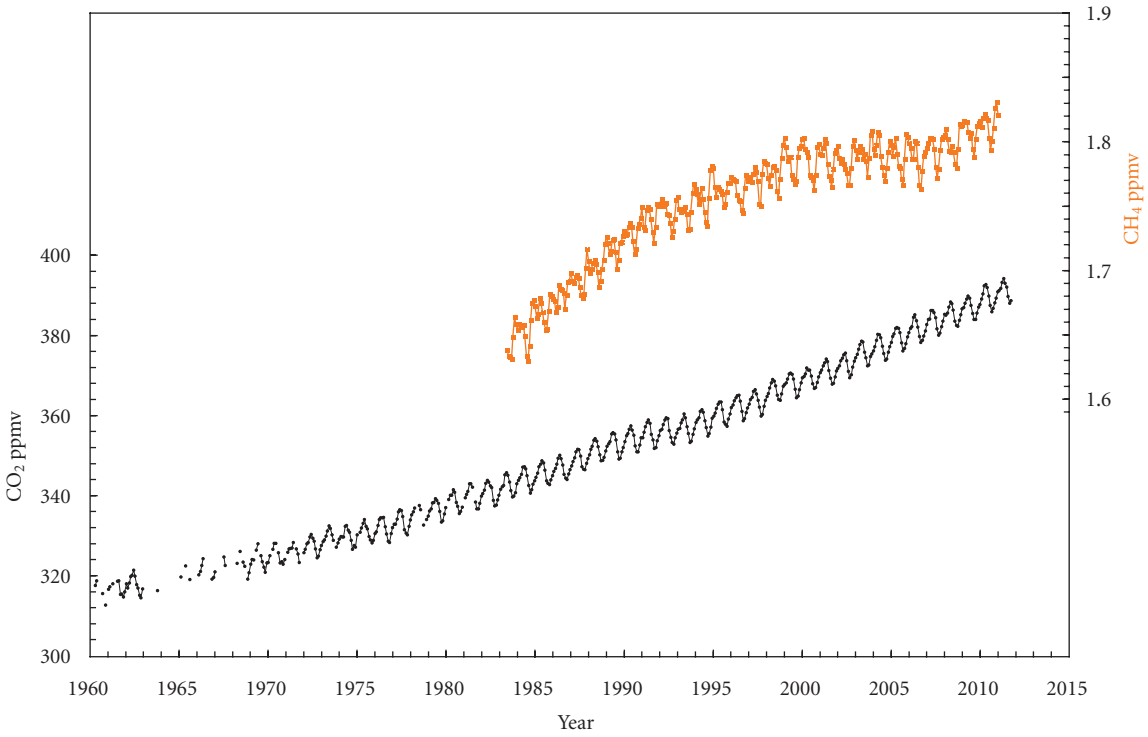

Figure 12.48 Concentrations of atmospheric CO_2 and CH_4 measured at the Scripps Institution of Oceanography Mauna Loa observatory over the last half-century. Sources: Scripps CO_2 program (http://scrippsco2.ucsd.edu) and NOAA Earth System Research Laboratory (http:// www.esrl.noaa.gov/gmd).

specific activity of 0, might be the answer. He and his colleague at the University of California San Diego, Roger Revelle, convinced another colleague, Charles Keeling, to begin measuring atmospheric CO_2 on a regular basis. Keeling soon set up a monitoring station atop Mauna Loa in Hawaii and, subsequently, one at the South Pole. Monthly measurements of atmospheric CO_2 have been made at these stations ever since; the data from Mauna Loa are shown in Figure 12.48. Superimposed on the wiggles caused by the seasonal cycle of photosynthesis in the terrestrial biosphere is a clear increase in atmospheric CO_2 from a seasonally adjusted value of 316 ppm in 1960 to 393 ppm in 2012, corresponding to an average annual increase of 1.5 ppm. The rate of rise has been increasing, however, and in the first decade of the 21st century approached 2 ppm per year. The increase in rate of rise is consistent with the increasing rate of emissions: the Intergovernmental Panel on Climate Change (IPCC) estimates that the carbon emitted by fossil-fuel burning increased from an average of 6.4 ± 0.4 gigatons of carbon (GtC) per year in the 1990s to 7.2 ± 3 GtC per year in 2000–2005 (Solomon *et al.*, 2007). In addition to fossil-fuel burning, the IPCC estimates that an additional 1.9 GtC per year is being added to the atmosphere through "land use change" (primarily cutting of tropic forests).

From the total emissions of around 9 GtC/yr, we would predict atmospheric CO_2 should be increasing by about 4 ppm per year, more than twice the actual rate. Put another way, the actual increase in atmospheric CO_2 is only around 4 GtC/yr. This difference reflects carbon transfer into other exogenous reservoirs shown in Figure 12.44. Various studies suggest the ocean is taking up about 2 GtC/yr. One consequence of this is ocean acidification: ocean surface pH has declined from an estimated preindustrial value of 8.17 to a present value of 8.07. The remaining 2–3 GtC/yr being released by fossil-fuel burning

and tropical deforestation is apparently being taken up by the northern hemisphere biosphere. There could be several reasons for the expansion of the northern hemisphere biosphere. First, as agriculture became more efficient in the 20th century, land cleared for agriculture has been abandoned and is returning to forest. Second, emissions from fossil-fuel burning, including both CO_2 and nitrates, may be stimulating growth. Third, warming is enabling expansion of boreal forests into regions previously covered by tundra.

Figure 12.48 also shows the change in atmospheric methane concentrations. These concentrations exceed the natural range of the last 650,000 years (320 to 790 ppb) as determined from ice cores. The principle anthropogenic sources are farm animals (ruminants such as cows and sheep) and rice farming. Other sources include landfills, sewage treatment facilities, biomass burning (incomplete burning produces methane as well as CO_2) and production and distribution of hydrocarbons (i.e., losses from oil and gas wells and distribution lines). In addition, warming may be enhancing release of methane from permafrost and methane clathrates on Arctic continental shelves.

Figure 12.49 shows annual globally-averaged land and ocean surface temperatures from 1890 to 2011. It is apparent that surface temperatures have increased over the period, albeit irregularly. The net increase is about 0.75°C. Most of that change has occurred since 1960 (the same year CO_2 measurements began); indeed the rate of increase over the last 50 years (0.13°C per decade) has been more than double the average rate of increase over the last 120 years. There are numerous other indicators of changing climate as well: the average temperature of the oceans has increased to depths of at least 3000 m (the ocean has been absorbing more than 80% of the heat added to the climate system); mountain glaciers have receded and snow and ice cover has declined, as has Arctic Sea ice (the latter dramatically); the average atmospheric water vapor content has increased (in a way more or less consistent with the extra water vapor that warmer air can hold); and sea-level has been rising at a rate of 1.8 mm/yr over the last 50 years. As the 2007 IPCC report put it, "*warming of the climate system is unequivocal*" (Solomon *et al.*, 2007).

In the previous sections, we saw how climate has changed over Earth's history and that these changes occurred as a result of changes to the carbon cycle and atmospheric greenhouse gas concentrations. Given what Earth's history teaches us, the observed recent climate change (Figure 12.49), the observed increase in greenhouse gas concentrations (Figure 12.48), and the known amounts of fossil fuels that have been burned, can we really question whether fossil-fuel burning is leading to climate change? The 2007 IPCC

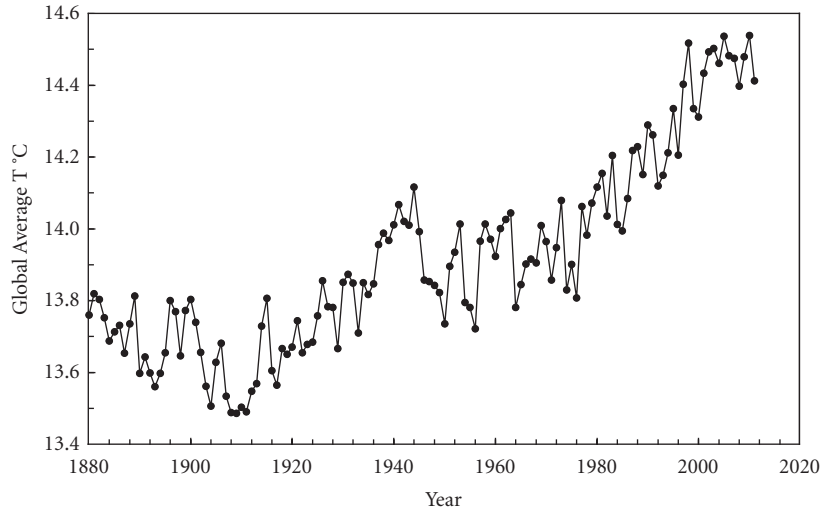

Figure 12.49 Annual globally averaged land and ocean surface temperatures since 1890. Source: US National Climate Data Center (http://www.ncdc.noaa.gov).

report (Solomon *et al*., 2007) puts it rather conservatively in saying: "*Most of the observed increase in global average temperatures since the mid-20th century is* very likely *due to the observed increase in anthropogenic greenhouse gas concentrations*." Climate change does have some "upside" effects, such as those noted by Arrhenius, but it is also has negative effects and the latter are likely to outweigh the former. Furthermore, our understanding of the climate system remains quite limited. There are reasons to think that temperature increases in the future might be more rapid than the present moderate rate (as an example, CO_2 solubility decreases with temperature, so the ocean may not take up as much CO_2 in the future). We have seen that in the Pleistocene, climate swung rapidly between cold and warm states. Our understanding of the Neoproterozoic "snowball Earth" episodes is far more limited, but climate modeling suggests the Earth oscillated rapidly between icehouse and hothouse states.

These observations should give us pause about the world's current equivocal, even cavalier, attitude toward climate change, and motivate us to move beyond fossil fuels as our principal energy source. Our fossil fuel reserves, while ultimately limited, remain vast, and we could continue to rely on them through much of this century and perhaps beyond. The Saudi oil minister once observed that the Stone Age did not end because people ran out of stones. What would it say about our modern society if the Fossil Fuel Age were to end only when we run out of fossil fuels? Promising technologies are available, and many of them are either now cost-effective or are approaching that point. Parts of the solution are relatively simple, such as becoming more energy-efficient and replacing coal with natural gas (the latter releases only half the CO_2 per joule energy produced) while we develop true carbon-free energy sources. Other parts may require ingenuity and some modest short-term sacrifice in return for much greater long-term benefit, but we must begin to earnestly strive to reach the goal of a carbon-free economy within the next few decades if we are to avoid severe disruption to our world.

REFERENCES AND SUGGESTIONS FOR FURTHER READING

Aiken, G.R., McKnight, D.M., Wershaw, R.L. and MacCarthy, P. (eds) 1985. *Humic Substances in Soil, Sediment, and Water*. New York, Wiley Interscience.

Arrhenius, S. 1896. Über den Einfluss des Atmosphärischen Kohlensäurengehalts auf die Temperatur der Erdoberfläche. *Proceedings of the Royal Swedish Academy of Science*, 22: 1–101.

Baars, O. and Croot, P.L. 2011. The speciation of dissolved zinc in the Atlantic sector of the Southern Ocean. *Deep Sea Research II*, 58: 2720–32.

Bartschat, B.M., Cabaniss, S.E. and Morel, F.M.M. 1992. Oligoelectrolyte model for cation binding by humic substances. *Environ. Sci. Technol.*, 26: 284–94.

Bennett, P.C. and Casey, W. 1994. Chemistry and mechanisms of low-temperature dissolution of silicates by organic acids, in *Organic Acids in Geological Processes* (eds E.D. Pitman and M.D. Lewan), pp. 162–200. Berlin, Springer Verlag.

Bergmann, W. 1978. *Zur Struckturaufklärung von Huminsäuren aus Abwasser*. PhD thesis, University of Tübingen.

Berner, R.A. 1981. *Early Diagenesis, A Theoretical Approach*. Princeton, Princeton University Press.

Berner, R.A. 1999. A new look at the long term carbon cycle. *GSA Today* 9(11): 1–6.

Berner, R.A. 2006. GEOCARBSULF: A combined model for Phanerozoic atmospheric O_2 and CO_2. *Geochimica et Cosmochimica Acta*, 70: 5653–64.

Berner, R.A. and Kothavala, Z. 2001. Geocarb III: a revised model of atmospheric CO_2 over Phanerozoic time. *American Journal of Science*, 301: 182–204. doi: 10.2475/ajs.301.2.182.

Berner, R.A., Lasaga, A.C. and Garrells, R.M. 1983. The carbonate-silicate geochemical cycle and its efffect on atmospheric carbon dioxide over the past 100 million years. *American Journal of Science*, 283: 641–83.

Boyle, E.A. 1988. The role of vertical chemical fractionation in controlling late Quaternary atmospheric carbon dioxide. *Journal of Geophysical Research*, 93: 701–15.

Buffle, J., Deladoey, P., Greter, F.L. and Haerdi, W. 1980. Study of the complex formation of copper (II) by humic and fulvic substances. *Analytica Chimica Acta*, 116: 255–74.

Cabaniss, S.E. and Shuman, M.S. 1988. Copper binding by dissolved organic matter: II. Variation in type and source of organic matter. *Geochimica et Cosmochimica Acta*, 52: 195–200.

Calvert, S.E. and Pederson, T.F. 1992. Organic carbon accumulation and preservation: how important is anoxia, in *Organic Matter: Productivity, Accumulation, and Preservation in Recent and Ancient Sediments* (eds J.K. Whelan and J.W. Farmington), pp. 231–63. New York, Columbia University Press.

Canfield, D.E. 2005. The early history of atmospheric oxygen: homage to Robert M. Garrels. *Annual Review of Earth and Planetary Science*, 33: 1–36. doi: doi:10.1146/annurev.earth.33.092203.122711.

Chiou, C.T., Freed, V.H., Schmedding, D.W. and Kohnert, R.L. 1977. Partition coefficient and bioaccumulation of selected organic chemicals. *Environmental Science and Technology*, 11: 475–8.

Chiou, C.T., Peters, L.J. and Freed, V.H. 1979. A physical concept of soil-water equilibria for nonionic organic compounds. *Science*, 206: 831–2.

Conkright, M.T. and Sackett, W.M. 1992. Stable carbon isotope changes during maturation of organic matter, in *Organic Matter: Productivity, Accumulation, and Preservation in Recent and Ancient Sediments* (eds J.K. Whelan and J.W. Farmington), pp. 403–14. New York, Columbia University Press.

de Leeuw, J.W. and Largeau, C. 1993. A review of the macromolecular organic compounds that comprise living organisms and their role in kerogen, coal, and petroleum formation, in *Organic Geochemistry: Principles and Applications* (eds M.H. Engel and S.A. Macko), pp. 23–72. New York, Plenum.

Deming, J.W. and Baross, J.A. 1993. The early diagenesis of organic matter: bacterial activity, in *Organic Geochemistry: Principles and Applications* (eds M.H. Engel and S.A. Macko), pp. 119–44. New York, Plenum.

Dominé, F., Bounaceur, R., Scacchi, G., *et al*. 2002. Up to what temperature is petroleum stable? New insights from a 5200 free radical reactions model. *Organic Geochemistry*, 33: 1487–99. doi: 10.1016/s0146-6380(02)00108-0.

Donat, J.R. and Bruland, K.W. 1993. A comparison of two voltametric techniques for determining zinc speciation in northeast Pacific Ocean water. *Marine Chemistry*, 28: 301–23.

Donnadieu, Y., Goddéris, Y., Ramstein, G., Nédelec, A. and Meert, J.G. 2004. Snowball Earth triggered by continental break-up through changes in runoff. *Nature*, 428: 303–6.

Drever, J.I. and Vance, G.F. 1994. Role of soil organic acids in mineral weathering processes, in *Organic Acids in Geological Processes* (eds E.D. Pitman and M.D. Lewan), pp. 138–61. Berlin, Springer Verlag.

Ellwood, M.J. 2004. Zinc and cadmium speciation in subantarctic waters east of New Zealand. *Marine Chemistry*, 87: 37–58. doi: 10.1016/j.marchem.2004.01.005.

Engel, M. and Macko, S.A. 1993. *Organic Geochemistry: Principles and Applications*. New York, Plenum Press.

Eyles, N. 2008. Glacio-epochs and the supercontinent cycle after ~3.0 Ga: Tectonic boundary conditions for glaciation. *Palaeogeography, Palaeoclimatology, Palaeoecology*, 258: 89–129. doi: 10.1016/j.palaeo.2007.09.021.

Falkowski, P., Scholes, R.J., Boyle, E., *et al*. 2000. The global carbon cycle: A test of our knowledge of Earth as a system. *Science*, 290: 291–6.

Fogel, M.L. and Cifuentes, M.L. 1993. Isotope fractionation during primary production, in *Organic Geochemistry: Principles and Applications* (eds M.H. Engel and S.A. Macko), pp. 73–98. New York, Plenum.

Fourier, J.-B.J. 1824. Remarques générales sur les températures du globe terrestre et des espaces planétaires. *Annales de Chimie et de Physique*, 27: 136–67.

Furrer, G. and Stumm, W. 1986. The coordination chemistry of weathering I. Dissolution kinetics of δ-Al_2O_3 and BeO. *Geochimica et Cosmochimica Acta*, 50: 1847–60.

Godderis, Y., Le Hir, G. and Donnadieu, Y. 2011. Modelling the Snowball Earth. *Geological Society London Memoirs*, 36: 151–61. doi: 10.1144/m36.10, 2011.

Graedel, T.E. and Crutzen, P.J. 1993. *Atmospheric Change: An Earth System Perspective*. New York, W.H. Freeman.

Grantham, P.J. and Wakefield, L.L. 1988. Variations in the sterane carbon number distributions of marine source rock derived crude oils through geological time. *Organic Geochemistry*, 12: 61–73. doi: 10.1016/0146-6380(88)90115-5.

Grauer, R. and Stumm, W. 1982. Die Koordinationschemie oxidisher Grenzflächen und ihre Auswirkung auf die Auflösingskinetic oxidisher Festphasen in wässrigen Lösungen. *Colloid. Polymer Science*, 260: 959–70.

Hansen, K.W. and Wallmann, K. 2003. Cretaceous and Cenozoic evolution of seawater composition, atmospheric O_2 and CO_2: A model perspective. *American Journal of Science*, 303: 94–148. doi: 10.2475/ajs.303.2.94.

Harvey, G.R. and Boran, D. 1985. Geochemistry of humic substances in seawater, in *Humic Substances in Soil, Sediment, and Water* (eds G.R. Aiken, D.M. McKnight, R.L. Wershaw and P. MacCarthy), pp. 233–47. New York, Wiley Interscience.

Hatcher, P.G. and Clifford, D.J. 1997. The organic geochemistry of coal: from plant materials to coal. *Organic Geochemistry*, 27: 251–74. doi: 10.1016/s0146-6380(97)00051-x.

Henrichs, S.M. 1993. Early diagenesis of organic matter: the dynamics (rates) of cycling of organic compounds, in *Organic Geochemistry: Principles and Applications* (eds M.H. Engel and S.A. Macko), pp. 101–17. New York, Plenum.

Hoefs, J. 1987. *Stable Isotope Geochemistry*. Berlin, Springer Verlag.

Hoffman, P.F., Kaufman, A.J., Halverson, G.P. and Schrag, D.P. 1998. A Neoproterozoic Snowball Earth. *Science*, 281: 1342–6. doi: 10.1126/science.281.5381.1342.